

# Uncertainty model for rate of change of frequency analysis with high renewable energy participation

**Tomas Rubiano, Mario A. Rios**

Department of Electrical and Electronics Engineering, School of Engineering, Universidad de los Andes, Bogota, Colombia

---

## Article Info

### Article history:

Received Jul 27, 2022

Revised Sep 9, 2022

Accepted Oct 1, 2022

---

### Keywords:

Frequency response

Grid-forming converters

Point estimate method

Rate of change of frequency

Synthetic inertia

---

## ABSTRACT

Large-scale integration of inverter-based renewables is displacing synchronous machine generation, causing a reduction in the inertia of electrical power systems. This reduction is reflected in an increase in the rate of change of frequency (RoCoF). Additionally, the variation of the RoCoF will depend on the uncertainty associated with the generation of non-conventional renewable energy sources. For the planning of the operation of the system, it is essential to know the range of variation of the RoCoF when there are disturbances in the system and uncertainties in the generation of non-conventional sources of renewable energy. This paper proposes to establish the calculation of a confidence interval of the RoCoF variation that considers these uncertainties. So, this paper proposes a method to consider these uncertainties based on the probabilistic point estimate method (PEM); considering multiple renewable non-conventional sources with correlated or uncorrelated behavior in their powers injected into the system. On the other hand, as there are different proposals to calculate the RoCoF, this paper presents the application of the uncertainty model with three different RoCoF proposed calculation methods.

*This is an open access article under the [CC BY-SA](https://creativecommons.org/licenses/by-sa/4.0/) license.*



---

## Corresponding Author:

Mario A. Rios

Department of Electrical and Electronics Engineering, School of Engineering, Universidad de los Andes

Cra 1 Este N° 19A-40, Edificio Mario Laserna ML-736, Bogota, Colombia

Email: mrios@uniandes.edu.co

---

## 1. INTRODUCTION

It is well known that inverter-based renewable energies, such as photovoltaic sources and wind power plants (WPPs), are beginning to displace inertia-providing synchronous machines (SMs) inside power grids. This trend is expected to grow as countries seek to reduce their carbon dioxide emissions. The rapid increase in the penetration of renewable energy sources poses numerous new challenges to transmission system operators (TSOs). Studies have begun in order to assess the impact of inertia loss in power systems and how to counteract it.

An important perspective is the analysis of the rate of change of frequency (RoCoF) following a power balance disturbance. The study of RoCoF is important for TSOs since they have to guarantee that frequency ancillary services can respond swiftly enough as to keep the frequency under preset boundaries. One of the main problems is that under-frequency may result in the need of load shedding, a condition highly undesirable for TSOs [1]. RoCoF is also important for generators, because high exposures could generate tripping and disconnection, reduce lifetime and in worst-case scenarios, put its structure and personnel at risk due to pole-slipping [2]. In cases of high renewable energy penetration, studies have shown that RoCoF could be an issue in weak networks when facing short-circuit faults [3]. RoCoF is becoming a pressing matter because there will be fewer available SMs left to connect themselves. As of yet, there is no global consensus on how RoCoF should be measured [2]. Its analysis needs to take distinct aspects into account. First, it is

unique to each bus found in the grid, due to the electric distance from SMs [4]. As stated in [2], there are several ways of measuring RoCoF, each of which will result in different values.

New literature has arisen in the last few years regarding how RoCoF can be counteracted and predicted, and how registered RoCoF data can lead to power system parameter estimations. Regarding RoCoF limitation, one of the main pillars is frequency control. In [5], a primary frequency control is proposed through a wide area measurement system (WAMS), where RoCoF sharing takes place. This paper also considers time delay, since frequency deviation requires swift but also accurate measurements. In [6], communication delays are also considered, but the frequency control is developed through optimal linear quadratic Gaussian control. Other methods have been proposed which do not need communication devices, mainly based on power imbalance estimation [7]. Some frequency controls have been established with an optimal artificial neural network controller, such as in [8]. This neural network is multi-layered with a specific training function. Similarly, Rozada *et al.* [9] implements load frequency control with deep multi-agent reinforcement learning recasting the load frequency control problem as a Markov decision process. In this sense, there is an ongoing academic discussion on how frequency controls can be constructed using various techniques in a way that RoCoF is greatly reduced.

RoCoF counteraction can be met with different ancillary services and backup reserves. Investigations have been wide on different possible solutions. In general, a rapid absorption or injection of power can decrease the size of the power imbalance, reducing frequency deviation. The way in which this energy can be rapidly stored or absorbed can be established through different means. Battery energy storage systems (BESSs) are a possible solution, as registered in [10]–[12]. Some papers, such as [13] have given a detailed description of the components, where BESSs have been developed using vanadium flow redox batteries. In [14], even electric vehicles have been mentioned as possible mechanisms for limiting RoCoF.

As has been said, RoCoF can also be used as a mean to estimate parameters of a given power system. For example, Yesil and Irmak [15] has registered a method for estimating the total power system connected inertia hourly through RoCoF measurements. In [16], RoCoF is calculated for a given scenario, and serves as a way to estimate the minimum inertia a system has to have in order to stay within stability limits. With the same estimating purpose, Wang *et al.* [17] presents RoCoF as a tool to calculate inertia support power.

RoCoF depends on the random power input from renewable energy generation, and as such, RoCoF should also be treated as a random variable. A Monte-Carlo approach would not be appropriate since exhaustive time and computational consumption would have to be spent on dealing with the mentioned aspects in each of the thousands of iterations. There is need of a more efficient way. Important ways of estimating RoCoF have been documented in [18], where a dynamic model has been tuned based on real past events. However, it is dependent on previous data acquisition, and the minimum amount of historical data and questions on the consideration of wind power plant (WPP) power input as a random variable are not clear. Tools for predicting RoCoF had been documented in [19] through deep learning techniques, were although predictions are similar to the recorded data, it is not clear how it will perform regarding undocumented RoCoF events that will take place. Some other estimation methodologies such as in [20] offer predictions based on costly computations, which are in the order of thousands of computations. In [21], the European platform named PLADYN was described, a platform for analyzing RoCoF behavior in European aggregation zones, functioning in islanding or interconnected mode. Although PALADYN has been validated with other simulation tools, is still does not consider WPP input as a random variable, so the results may not be adequate for power system planning.

This paper proposes a point estimate method (PEM) based probabilistic analysis of RoCoF, and it is applied to the IEEE 9 bus system. The aim is to describe the behavior of RoCoF in terms of a confidence interval for any possible operation point. The PEM  $2m+1$  method developed by Hong [22] was used. With PEM, a small number of iterations suffice to obtain a reliable description of the given random variable. Another of its advantages is that it allows the correlation between WPPs to be considered. For example, in [20], 8,760 dispatches had to be computed in order to evaluate RoCoF through hourly dispatches. Through PEM, this amount can be greatly reduced even if there are many WPPs. Another of its advantages is that it allows the correlation between WPPs to be considered. The value of this new method, as will be discussed further, is its use of confidence intervals as a way of comparing between different cases, topologies, control methods. These confidence intervals can also be easily used for power system planning and decision-taking. They can be thought of as a “normalized” approach for comparing RoCoF performance.

This paper has been organized as: section 1 presents the RoCoF definition and computation alternatives used in this paper. In addition, section 2 presents the proposal for computing the RoCoF considering uncertainties of renewable energy sources for both cases: uncorrelated and correlated sources. Section 3 shows the results of RoCoF assessment in the test system (9-bus system). Finally, section 4 presents the conclusions of this paper.

## 2. METHOD

The RoCoF is the change rate of the frequency after a disturbance occurs in the power system [23]; as disturbances are the disconnection of a generator, load disconnection, among others. With the integration of non-conventional renewable sources, the power system experiments a reduction of its inertia [5]. By system inertia can be understood as the capacity of the system that prevents the variation of the system frequency and is proportional to the sum of the kinetic energies of all the (synchronous) generators of the system [24]. This section presents a proposed method for developing a probabilistic RoCoF assessment. Initially, three RoCoF computation methods are formulated, then a probabilistic method for computing RoCoF for a single non-conventional resource is proposed. Then, an assessment method for non-conventional renewable sources (RES), like wind and solar.

### 2.1. RoCoF computation

There are no international standards as to how RoCoF should be measured. EirGrid, Ireland's TSO, regulates that RoCoF should be measured at 500 ms, since at this time generators return to a coherent state [25]. EirGrid also introduces as per its own graph the RoCoF measurement as an averaging. This means this value can be taken as: frequency value/elapsed time.

Several considerations arise regarding the effects that measurement techniques have on the RoCoF value. Measuring RoCoF as an averaging can lead to inaccuracies, since it does not capture the slope of the tangent at that point. In the same way, measuring at 500 ms can obviate larger RoCoF values to which generators and system relays are exposed [26]. As a response, this paper will consider the use of a numerical equation which calculates the derivative of frequency, the slope of the tangent line. This will be done through the 5-point formula [27]. If data at both sides is available, the formula uses the midpoint of the interval as (1),

$$f'(x_0) = \frac{1}{12h} [f(x_0 - 2h) - 8f(x_0 - h) + 8f(x_0 + h) - f(x_0 + 2h)] \quad (1)$$

where  $h$  is the time spacing between each point. If that is not the case, the following expression can be used when data for the lower limit edge-point is given:

$$f'(x_0) = \frac{1}{12h} [-25f(x_0) + 48f(x_0 + h) - 36f(x_0 + 2h) + 16f(x_0 + 3h) - 3f(x_0 + 4h)] \quad (2)$$

For upper limit edge-points,  $h$  can be replaced with  $-h$ .

With the motivation being to highlight differences coming from decisions to use a specific time (500 ms) and/or averaging or not, the following three methodologies of measurement of the RoCoF have been proposed:

- The RoCoF value as the highest calculation with the 5-point formula. It will be represented with *Max 5p* or *Max 5 Point*.
- The RoCoF value as the derivative at 500 ms with the 5-point formula. Its representation will be through *5p* or *5 Point* at 500 ms.
- The RoCoF value as 500 ms measured through averaging. It will be mentioned with *Avg*.

### 2.2. RoCoF assessment for a single source

A first case of study is to compute the RoCoF for a power system with a single WPP using the PEM method. The  $2m+1$  PEM developed by Hong [22] requires the knowledge of the first 5 central moments of the random variable  $(\mu_p, \sigma_p, \lambda_{X,3}, \lambda_{X,4}, \lambda_{X,5})$  for a successful implementation. For the PEM application, the RoCoF will be a random variable function wind power injection, called  $Z$ .

Let  $Z$  be a random variable function of the random variable  $X$  (the wind power injection),  $Z=h(X)$ . In this case,  $X$  is a 1-dimensional vector. The first and second moments of  $Z$  can be computed as (3) and (4),

$$\mu_z = \sum_{i=1}^{2m+1} w_i h(x_i) \quad (3)$$

$$E(Z^2) = \sum_{i=1}^{2m+1} w_i h^2(x_i) \quad (4)$$

which allows the calculation of  $\sigma_z = \sqrt{E(Z^2) - \mu_z^2}$ . In (3) and (4),  $x_i$  denotes a point concentration and  $p_i$  its matching weight. Each point concentration is defined as  $x_i = \mu_z + \xi_i \sigma_z$ . Each concentration point has a weight given by (5),

$$w_i = \frac{\xi_j \xi_{k+1}}{(\xi_j - \xi_i)(\xi_k - \xi_i)} \quad (5)$$

where  $i, j, k = 1, 2, 3$  and  $i \neq j \neq k$ . And  $\xi_1, \xi_2$  and  $\xi_3$  are the roots of the following polynomial:

$$d_3 \xi^3 + d_2 \xi^2 + d_1 \xi + d_0 = 0 \tag{6}$$

where the coefficients are defined by (7), (8), (9), and (10):

$$d_0 = \lambda_{x,5} - \lambda_{x,3}(2\lambda_{x,4} - \lambda_{x,3}^2) \tag{7}$$

$$d_1 = \lambda_{x,3}(\lambda_{x,5} - \lambda_{x,3}) + \lambda_{x,4}(1 - \lambda_{x,4}) \tag{8}$$

$$d_2 = \lambda_{x,3}(\lambda_{x,4} + 1) \tag{9}$$

$$d_3 = \lambda_{x,4} - (1 + \lambda_{x,3}^2)^2 \tag{10}$$

**2.3. RoCoF assessment for  $m$  renewable sources**

The assessment of the RoCoF for a power system with multiple renewable sources ( $m$ ) can be made using the  $2m+1$  PEM method including correlated behavior between them. Detailed information on this process can be found in [22], [28]–[30]. For a successful implementation, the first four central moments of each random variable (each renewable source) are required ( $\mu_{pl}, \sigma_{pl}, \lambda_{pl,3}, \lambda_{pl,4}$ ).

As in the case for one variable, the main objective is to calculate the first and second moment of  $Z$ , in this case the RoCoF. The evaluation of a point concentration involves setting the other variables at their mean value. Similar to the single source PEM,  $x_{l,k} = \mu_l + \xi_{l,k} \sigma_{pl-1}$ .  $Z$  can be defined as (11).

$$Z(l, k) = F(\mu_{p1}, \dots, \mu_{pl-1}, x_{l,k}, \mu_{pl+1}, \dots, \mu_{pm}) \tag{11}$$

The first and second moments of  $Z$  (in this case, the RoCoF) can be calculated as (12) and (13).

$$\mu_z = \sum_{l=1}^m \sum_{k=1}^{2m+1} w_{l,k} Z(l, k) \tag{12}$$

$$E(Z^2) = \sum_{l=1}^m \sum_{k=1}^{2m+1} w_{l,k} Z^2(l, k) \tag{13}$$

The standard deviation of the RoCoF can be calculated as  $\sigma_z = \sqrt{E(Z^2) - \mu_z^2}$ .

For the commencement of the PEM ( $2m+1$ ) for  $m$  variables, the correlated variables must be first decorrelated based on fictitious variables. The covariance matrix of correlated variables  $C_p$  (injected power of renewable sources) has to be constructed using unit values, and is given as (14):

$$C_p = \begin{pmatrix} \sigma_{p1}^2 & \sigma_{p1p2} & \dots & \sigma_{p1pm} \\ \sigma_{p2p1} & \sigma_{p2}^2 & \dots & \sigma_{p2pm} \\ \vdots & \vdots & \ddots & \vdots \\ \sigma_{pm p1} & \sigma_{pm p2} & \dots & \sigma_{pm}^2 \end{pmatrix} \tag{14}$$

where  $\sigma_{pipj} = r_{pipj} \times \sigma_{pi}^2 \times \sigma_{pj}^2$  and  $r_{pipj}$  are the correlation between the random variables  $i$  and  $j$  (i.e the injected power of wind and renewables sources). A lower diagonal matrix  $L$  can be completed from  $C_p$  through the Cholesky transformation.

$$[C_p] = [L][L^T] \tag{15}$$

The vector of injected power by renewable sources  $[p] = [p_1, \dots, p_m]$  contains all the  $m$  random variables. The auxiliary uncorrelated variables  $[x] = [x_1, \dots, x_m]$  have to be constructed. The central moments of  $[x]$  are calculated from (16) to (19).

$$[\mu_x] = [L^{-1}][\mu_p] \tag{16}$$

$$[C_x] = [L]^{-1}[C_p][[L]^{-1}]^T = [I] \tag{17}$$

$$\lambda_{x,3} = \sum_{r=1}^m ([L^{-1}]_{l,r})^3 \lambda_{p,3} \sigma_p^3 \tag{18}$$

$$\lambda_{x_{l,4}} = \sum_{r=1}^m ([L^{-1}]_{l,r})^4 \lambda_{p,4} \sigma_p^4 \quad (19)$$

Still inside the “non-correlated space”, the point concentrations and their corresponding probability concentrations have to be computed. The former is defined as  $x_{l,k} = \mu_{x,l} + \xi_{l,k} \sigma_{x,l}$  with  $l = 1, \dots, m$  and  $k = 1, \dots, 2m + 1$ . These can be calculated as (20).

$$\xi_{l,k} = \begin{cases} \frac{\lambda_{x_{l,3}}}{2} + (-1)^{3-k} \sqrt{\lambda_{x_{l,4}} - \frac{3}{4} \lambda_{x_{l,3}}^2}, & k = 1, 2 \\ 0, & k = 3 \end{cases} \quad (20)$$

The corresponding weights for each point concentration are:

$$w_{l,k} = \frac{(-1)^{3-k}}{\xi_{l,k} (\xi_{l,1} - \xi_{l,2})}, \quad k = 1, 2 \quad (21)$$

$$w_{l,3} = \frac{1}{m} - \frac{1}{(\lambda_{x_{l,4}} - \lambda_{x_{l,3}}^2)^2} \quad (22)$$

With these point concentrations and each of their weights, the uncorrelated variables are organized according to (11). Purpose being to allow matrix multiplications in (24), these can be arranged in a  $m \times 2m + 1$  matrix. For this specific two variable  $2m+1$  PEM case:

$$[x] = \begin{bmatrix} x_{1,1} & x_{1,2} & x_{1,3} & x_{1,3} & x_{1,3} \\ x_{2,3} & x_{2,3} & x_{2,3} & x_{2,1} & x_{2,2} \end{bmatrix} \quad (1)$$

the concentration points being transformed back to the correlated space are calculated as (24).

$$[p] = [L][x] \quad (2)$$

The described step in (24) may result in some point concentrations outside feasible limits, in this case compute the limit which is exceeded. The same weights of the point concentrations are kept. Being back in the correlated space, (12) and (13) can now be used with the values calculated in (24) [29]. It is important to bear in mind that this is a general method for correlated variables. For such scenarios where the variables are uncorrelated, (20), (21) and (22) can be used without any transformation of both the variables and their central moments.

#### 2.4. Confidence intervals

As previously stated, (3) and (4) or (12) and (13) will allow us to calculate  $\mu_z$  and  $\sigma_z$ . However, the performance assessment of the system's RoCoF is not enough to be based on the average value; for such assessment, it is proposed to use the confidence interval. The confidence interval gives to the analyst information about the range of the frequency deviation as function of wind farm's power injection uncertainty. The confidence interval with a confidence level of 95% for  $Z$  can be computed as in (25) [31].

$$P(\mu_z - 1.96 \times \sigma_z < Z < \mu_z + 1.96 \times \sigma_z) = 0.95 \quad (3)$$

#### 2.5. Grid-forming converter model

Grid-forming (GFR) converters arise as possible solutions to mitigate RoCoF related problems. These power converters have a control loop that enables them to establish their own voltage reference [32]. GFR converters can operate according to different control system configurations. As such, they can operate as fast frequency response (FFR) or as synthetic inertia providers. The difference between them is worth highlighting. FFR is regarded as a fast power reaction, either by injecting or absorbing power based on any frequency deviation. Synthetic inertia also provides this service, as well as mimicking a SM's rotational mass response, such as the swing equation, and as such is proportional to RoCoF [11]. The GFR parameters can be set allowing the damping factor to be adjusted during the event. Another advantage of these converters is that their response is not degraded by measurement delays of frequency and RoCoF [33].

This paper will use a GFR converter which provides synthetic inertia, called a virtual synchronous generator (VSG) [34]. This model has been chosen because it allows coupling and parallel operation with real SMs, including load sharing. As such, it is an appropriate choice for the tests cases that will be selected. A detailed description of its components, such as AVR, droop, governor-control and virtual impedance is found in [34].

**3. RESULTS AND DISCUSSION**

**3.1. Test system**

Modifications of the 9-Bus system [35] was used for the analysis of frequency dynamic behavior. Two different cases are considered. The first case considers one WPP as shown in Figure 1, which has 250 MW as rated power. This value was chosen as to set it close to the 1st SM's rated power, and because of the low plant factors of WPPs [11]. The second test system of Figure 2 includes two WPPs, WPP1 and WPP2, the former with 250 MW and the latter with 262 MW rated power.

For both cases, the power output of the SM at bus 1 will be held at 49.6 MW, approximately 20% of its rated power. For the VSG model an inertia constant H is defined. This value will be chosen as H=2.34 s, corresponding to the replaced SM's inertia constant of the test system [35]. SM 1 will have an inertia corresponding to H=9.55 s. For the first case, SM 2 will have H=3.33 s.

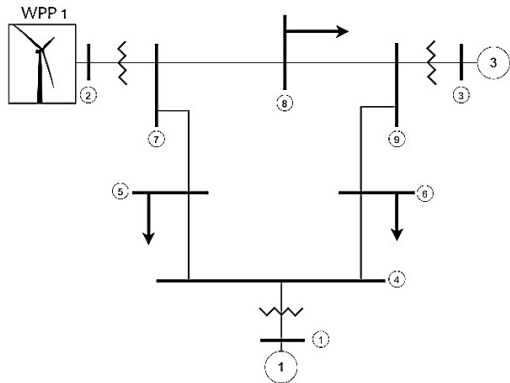


Figure 1. Test system 9 bus system with one WPP

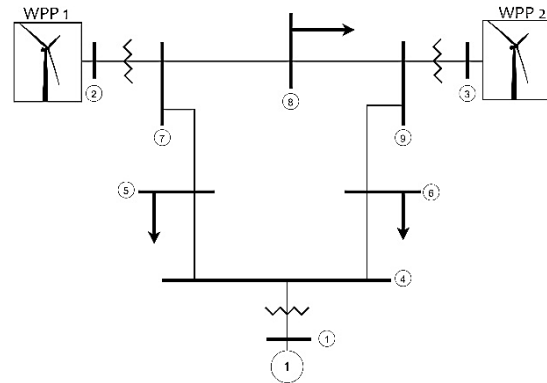


Figure 2. Test system 9 bus system with two WPP

**3.1.1. Selected disturbance**

RoCoF takes place when a power balance disturbance takes place in the power system. According to [32], many TSO's are analyzing a maximum power unbalance corresponding to 10% of the minimum load. Inside the IEEE 9-Bus system this corresponds to a load of 31.5 MW+11.5 MVar. This will be the amount of power that will be used for both load and generation loss disturbances. Regarding this disturbance, it is important to make a distinction between a loss of load and a loss of generation. Even though both create a power unbalance of the same magnitude, the latter involves loss of synchronous inertia. Because of this, simulations will be carried both for loss of load and loss of generation.

**3.1.2. Wind power plant parameters**

As section 2 mentions, the central moments of the WPPs are needed to successfully implement the  $2m+1$  PEM algorithm. In study [36], a WPP of nominal power  $P_n$  is characterized through a Monte-Carlo simulation; showing the plant factor ( $\mu_p/P_n$ ) is equal to 0.3018 while the coefficient of variation ( $\sigma_p/\mu_p$ ) equal to 1.009. As, it can be appreciated, it shows a large dispersion in the injected power. Based on simulated data from [36], the skewness and kurtosis are computed and presented in Table 1. The study cases reported in this paper have parameters corresponding to the central moment values presented at Table 1 ( $\mu_p/P_n$ ,  $\sigma_p/P_n$ ,  $\lambda_{p,3}$ ,  $\lambda_{p,4}$ ,  $\lambda_{p,5}$ ).

Table 1. WPP normalized central moments

| Central Moment  | Value  |
|-----------------|--------|
| $\mu_p/P_n$     | 0.3018 |
| $\sigma_p/P_n$  | 0.3046 |
| $\lambda_{p,3}$ | 0.849  |
| $\lambda_{p,4}$ | 2.427  |
| $\lambda_{p,5}$ | 3.939  |

**3.2. Case 1: one WPP**

The first case assumes there is only one WPP of 250 MW rated power. Thus, based on normalized central moments defined at Table 1, the mean value of the injected power is 75.45 MW, the standard deviation is 76.15 MW. The PEM method uses the normalized  $\lambda_{p,3}$ ,  $\lambda_{p,4}$ ,  $\lambda_{p,5}$  given by Table 1 for this case.

Table 2 shows the three concentration points required to model uncertainties of the WPP for the RoCoF computation, following the PEM ( $2m+1$ ) procedure explained at section 2.2. The weight factor of each concentration point is computed using (5).

Table 2. Case 1-concentration points

| Concentration point | Injected power [MW] | Weight factor |
|---------------------|---------------------|---------------|
| 1                   | 11.7                | 0.5167        |
| 2                   | 104.3               | 0.3215        |
| 3                   | 220.8               | 0.1618        |

As mentioned in the section 2.1, the RoCoF value will be calculated from three different methods (identified as 5p, Avg., Max 5p.) in order to evaluate the differences among them. Table 3 presents the RoCoF computed for each concentration point (given by its injected power) by the three different methods for two disturbances: i) loss of load of 31.5 MW and ii) loss of generation of 31.5 MW. As, it is expected, the frequency increases when a loss of load occurs, and decreases when a loss of generation happens. However, it is noted the results of the RoCoF are different by each method. Another interesting result is that the RoCoF for a loss of load increases when the WPP injected power is larger; but, in the loss of generation case the absolute value of the RoCoF increases lightly. Finally, the two simulated disturbances are of the same magnitude; as it is observed, the frequency change is larger for loss of generation than for the loss of load (absolute value comparison).

Table 3. Case 1-ROCOF according to computation method and disturbance

| WPP1 Power [MW] |         | RoCoF [Hz/s] Load Loss |         | RoCoF [Hz/s] Gen. Loss |
|-----------------|---------|------------------------|---------|------------------------|
| 11.7            | 5p      | 0.186                  | 5p      | -0.349                 |
|                 | Avg.    | 0.240                  | Avg.    | -0.356                 |
|                 | Max 5p. | 0.288                  | Max 5p. | -0.420                 |
| 104.3           | 5p      | 0.217                  | 5p      | -0.357                 |
|                 | Avg.    | 0.268                  | Avg.    | -0.360                 |
|                 | Max 5p. | 0.315                  | Max 5p. | -0.427                 |
| 220.8           | 5p      | 0.249                  | 5p      | -0.365                 |
|                 | Avg.    | 0.295                  | Avg.    | -0.363                 |
|                 | Max 5p. | 0.338                  | Max 5p. | -0.437                 |

Table 4 presents the weighted RoCoF ( $\mu_z$ ) computed from the results of each concentration point and disturbance type presented at Table 3. Also, Table 4 shows the standard deviation of the RoCoF ( $\sigma_z$ ) for each disturbance (loss of load or loss of generation). Also, it is presented the confidence interval of the RoCoF for a confidence level of 95%. Considering the uncertainty behavior of the injected power of a WPP, it is observed that the RoCoF for loss of load has a confidence interval around the average value between 12% and 21% (according to the computation method); while for the loss of generation, the confidence interval around the average value is between 4% and 9% (according to the computation method).

Table 4. Case 1-mean value, stand. dev. and 95% confidence interval

| Item         | Disturb. Type | 5 Points at 0.5 s | Average at 0.5 s | Max Value 5 Points |
|--------------|---------------|-------------------|------------------|--------------------|
| $\mu_z$      | Load Loss     | 0.206             | 0.258            | 0.305              |
|              | Gen Loss      | -0.354            | -0.358           | -0.425             |
| $\sigma_z$   | Load Loss     | 0.023             | 0.0205           | 0.019              |
|              | Gen Loss      | 0.006             | 0.0030           | 0.006              |
| 95% Interval | Load Loss     | (0.16, 0.25)      | (0.22, 0.30)     | (0.27, 0.34)       |
|              | Gen Loss      | (-0.342, -0.367)  | (-0.391, -0.380) | (-0.44, -0.41)     |

### 3.3. Case 2: two WPP

As Figure 2 shows, case 2 includes two WPP, one of 250 MW rated power connected at node 2 and the second one of 260 MW rated power connected at node 3. Table 5 shows the concentration points and their weights which result from the application of PEM ( $2m+1$ ) explained at section 2.3. For this case, three scenarios will be taken under consideration according to the assumed correlation factor between injected powers of WPP1 and WPP2. These correlations are  $r_{p_1p_2} = 0, 0.2, -0.2$ .

Table 5. Case 2-concentration points

| Scenario             | Concentration point | Injected power | Scenario | Concentration point |
|----------------------|---------------------|----------------|----------|---------------------|
| $r_{p_1 p_2} = 0$    | 1                   | 3.2            | 79.2     | 0.3836              |
|                      | 2                   | 212.1          | 79.2     | 0.2015              |
|                      | 3                   | 75.3           | 79.2     | -0.1722             |
|                      | 4                   | 75.3           | 3.3      | 0.3836              |
|                      | 5                   | 75.3           | 223      | 0.2025              |
| $r_{p_1 p_2} = 0.2$  | 1                   | 3.2            | 64       | 0.3836              |
|                      | 2                   | 212.1          | 107.9    | 0.2025              |
|                      | 3                   | 75.3           | 2.5      | 0.3578              |
|                      | 4                   | 75.3           | 226.1    | 0.1869              |
|                      | 5                   | 75.3           | 79.2     | -0.1308             |
| $r_{p_1 p_2} = -0.2$ | 1                   | 3.2            | 94.4     | 0.3836              |
|                      | 2                   | 212.1          | 50.4     | 0.2025              |
|                      | 3                   | 75.3           | 3.6      | 0.3648              |
|                      | 4                   | 75.3           | 226.1    | 0.1878              |
|                      | 5                   | 75.3           | 79.2     | -0.1386             |

For the first scenario ( $r_{p_1,p_2}=0$ ) the third concentration point corresponds to the point formed by the mean value of the injected powers at WPP1 and WPP2, while for another scenarios the fifth concentration point is the mean value of the injected powers at WPP1 and WPP2. In each scenario, the other concentrations points are the combinations obtained by application of the PEM method. Table 6 contains the RoCoF results after evaluation in every concentration point, as defined in (11); while Table 7 presents the confidence intervals of the RoCoF. These tables include comparison of the results of the RoCoF obtained by the three methods of computation under study in this paper.

Table 6. Case 2-ROCOF according to computation method, disturbance, and correlation

| Scenario             | Concentration point | Injected power WPP1 [MW] | Injected power WPP2 [MW] | RoCoF [Hz/s]              |          | RoCoF [Hz/s] Averaging Method at 500 ms |          | RoCoF [Hz/s] Max 5 point formula |          |
|----------------------|---------------------|--------------------------|--------------------------|---------------------------|----------|---|----------|----------------------------------|----------|
|                      |                     |                          |                          | 5 Point formula at 500 ms |          | Load loss                               | Gen loss | Load loss                        | Gen loss |
|                      |                     |                          |                          | Load loss                 | Gen loss |   |          |                                  |          |
| $r_{p_1 p_2} = 0$    | 1                   | 3.2                      | 79.2                     | 0.1780                    | -0.3361  | 0.2669                                  | -0.3361  | 0.3647                           | -0.4031  |
|                      | 2                   | 212.1                    | 79.2                     | 0.2215                    | -0.3478  | 0.2971                                  | -0.3751  | 0.3862                           | -0.4150  |
|                      | 3                   | 75.3                     | 79.2                     | 0.1930                    | -0.3399  | 0.2769                                  | -0.3399  | 0.3762                           | -0.4063  |
|                      | 4                   | 75.3                     | 3.3                      | 0.1825                    | -0.3390  | 0.2730                                  | -0.3697  | 0.3756                           | -0.4030  |
|                      | 5                   | 75.3                     | 223                      | 0.2290                    | -0.3420  | 0.2895                                  | -0.3668  | 0.3662                           | -0.4149  |
| $r_{p_1 p_2} = 0.2$  | 1                   | 3.2                      | 64                       | 0.1754                    | -0.3355  | 0.2652                                  | -0.3662  | 0.3641                           | -0.4026  |
|                      | 2                   | 212.1                    | 107.9                    | 0.2291                    | -0.3474  | 0.2986                                  | -0.3744  | 0.3832                           | -0.4150  |
|                      | 3                   | 75.3                     | 2.5                      | 0.1825                    | -0.3390  | 0.2730                                  | -0.3697  | 0.3756                           | -0.4030  |
|                      | 4                   | 75.3                     | 226.1                    | 0.2300                    | -0.3420  | 0.2896                                  | -0.3667  | 0.3656                           | -0.4149  |
|                      | 5                   | 75.3                     | 79.2                     | 0.1930                    | -0.3399  | 0.2796                                  | -0.3695  | 0.3762                           | -0.4063  |
| $r_{p_1 p_2} = -0.2$ | 1                   | 3.2                      | 94.4                     | 0.1804                    | -0.3360  | 0.2686                                  | -0.3660  | 0.3652                           | -0.4037  |
|                      | 2                   | 212.1                    | 50.4                     | 0.2149                    | -0.3484  | 0.2956                                  | -0.3758  | 0.3886                           | -0.4144  |
|                      | 3                   | 75.3                     | 3.6                      | 0.1825                    | -0.3390  | 0.2731                                  | -0.3697  | 0.3756                           | -0.4030  |
|                      | 4                   | 75.3                     | 226.1                    | 0.2300                    | -0.3420  | 0.2896                                  | -0.3667  | 0.3656                           | -0.4149  |
|                      | 5                   | 75.3                     | 79.2                     | 0.1930                    | -0.3399  | 0.2796                                  | -0.3695  | 0.3762                           | -0.4036  |

Table 7. Case 2-95% confidence interval

| Scenario             | Method      | Load loss      | Gen. loss        |
|----------------------|-------------|----------------|------------------|
| $r_{p_1 p_2} = 0$    | 5 Point     | (0.149,0.243)  | (-0.363, -0.317) |
|                      | Avg.        | (0.248,0.308)  | (-0.382, -0.365) |
|                      | Max 5 point | (0.343,0.399)  | (-0.435, -0.379) |
| $r_{p_1 p_2} = 0.2$  | 5 Point     | (0.146,0.247)  | (-0.349, -0.331) |
|                      | Avg.        | (0.251, 0.303) | (-0.375, -0.363) |
|                      | Max 5 point | (0.356,0.386)  | (-0.419, -0.395) |
| $r_{p_1 p_2} = -0.2$ | 5 Point     | (0.154,0.237)  | (-0.346, -0.334) |
|                      | Avg.        | (0.257,0.300)  | (-0.370, -0.368) |
|                      | Max 5 point | (0.356,0.389)  | (-0.415, -0.400) |

### 3.4. Analysis and discussion

As section 2.4 proposes, the main idea to capture the uncertainty of injected powers by non-conventional renewable sources is to define a 95% confidence interval. Based on results presented a Tables 3, 4, and Figure 3 contains the final 95% confidence intervals for cases 1 and 2, and for the three study scenarios of case 2. Regarding both the one WPP and two WPPs cases, for all three RoCoF

measurement methods the scenario with generation loss had slightly larger absolute values than those scenarios with load loss; however, the uncertainty (size of the confidence interval) is lower when a loss of generation occurs than when a loss of load happens. The larger sensitivity of the frequency variation to loss of generation compared to the loss of load is due to the fact that generation loss also involves loss of synchronous inertia, which according to [32], is the primary limitation to high RoCoF values. In the loss of load case, there is not a loss of synchronous inertia. Nevertheless, intervals for generation loss are thinner than those for load loss, evidently wider. These lays an important burden on perturbation location, where generation loss is close to SM1 (load loss takes place in another bus), where the electrical distance to SMs could be playing a role on RoCoF being less variable.

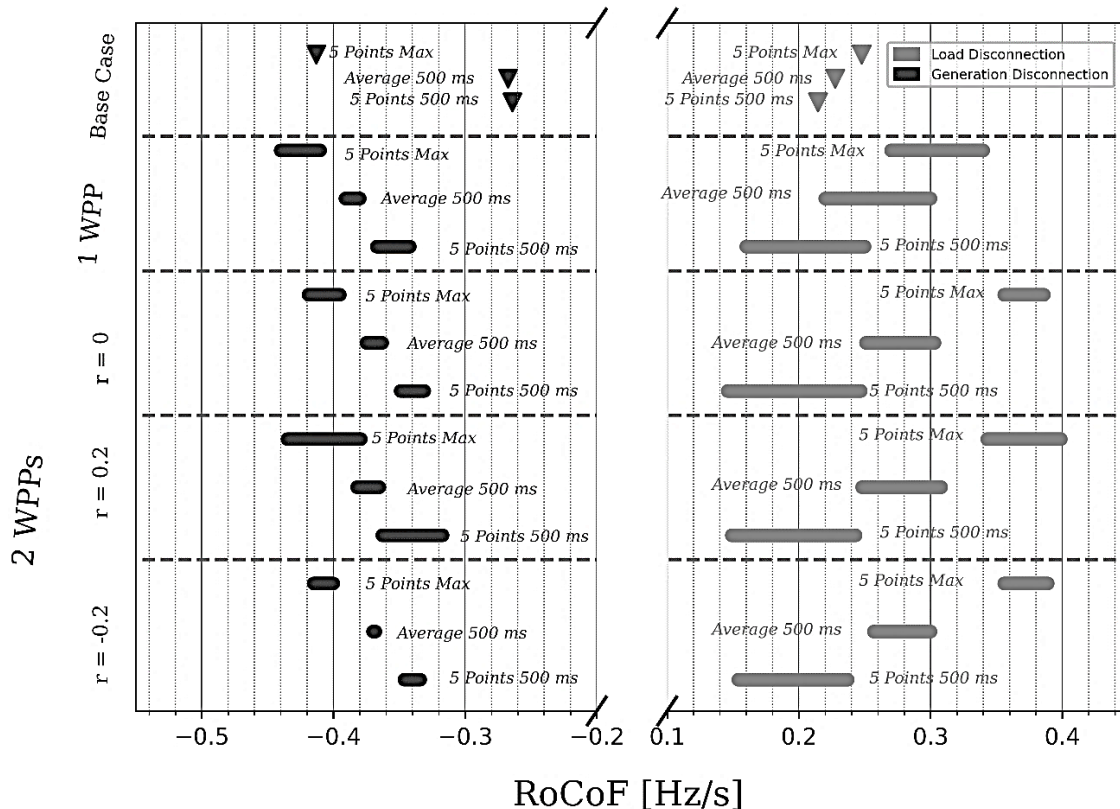


Figure 3. Confidence intervals (95%) for all cases and scenarios

Figure 3 contains the “base case” of the original system presented at [35], with all three SM and their inertias. RoCoF is in this base case deterministic since there are no WPPs. It can be seen that these values are not widely separated from the intervals, explained by SM 2 only having 13% of total system inertia. In addition, it is shown that when WPP are in the system (instead of synchronous machines) the RoCoF increases as it is expected.

Case 2 offers important remarks as to understand if the GFR converter is fulfilling its job or not. Comparing the case 3 with case 1, all intervals with matching measurement method are located very close, which means that the GFR converter is mimicking the SM in an effective way. Another interesting result of case 2 is around the correlation among WPP sources. When the correlation is positive the confidence intervals are larger than when the WPP sources are statistically independent (correlation  $r=0$ ). By contrast, when the WPP has a negative correlation behavior the confidence intervals are shorter than the scenario of statistically independent WPPs. This fact could be profited by system operators in order to use WPP without affecting too dramatically the RoCoF of the system.

RoCoF is not critically dependent on the operating set point from both SMs and power converters. RoCoF is mainly affected by the amount of inertia connected to the system, not by its amount of power output. The correlation between WPPs does not have a direct incidence on the final 95% confidence interval. In this sense, results will only vary slightly as the correlation between them changes.

The use of these confidence intervals as a common platform for comparing RoCoF behavior was successful allowing the comparison between different number of connected WPP and different correlations between them. This methodology can be further used for an adequate comparison on common grounds between different network topologies and different installed capacities. For example, grids with high impedance networks and low redundancy under N-1 contingencies are more prone to experience RoCoF issues [37], and their performance can be directly compared with other networks through the 95% confidence intervals, since they can be seen as a “normalized” tool on a common base. It could also even be expanded to compare RoCoF values through different primary control schemes.

Finally, this paper has offered critical information regarding RoCoF measurement methodologies. EirGrid [25] has been one of the first TSOs to implement in its regulation RoCoF definitions. Still, to reach an international consensus, it is important to understand what is being lost and gained by averaging, and by selecting only one specific time to measure.

Figure 3 shows the importance to define the computation method of the RoCoF. The average method (*Avg.* as it has been identified in this paper) proposed by EirGrid is a good indicator to show that RoCoF (absolute value) increases when WPP are placed at the system. However, it sub estimates the actual value of the RoCoF. By contrast, the RoCoF value as the highest calculation with the 5-point formula (identified as *Max 5p* or *Max 5 Point* in this paper) gives a more precise value of the actual value of the RoCoF.

Figure 4 gives another comparison of the RoCoF values computed by the three methods studied in this paper. Figure 4 presents the RoCoF behavior for two cases: i) a load disconnection and ii) a generation disconnection. Simultaneously, for each case, the RoCoF is computed using two different methods. The continuous line (for each case) is computed using the *5-point* formula, while the dot's line is computed by using the method of averaging.

As, Figure 4 shows, the maximum value of RoCoF is not the same point for the method of *5-points* formula and the averaging method. Averaging is also masking higher RoCoF values. As such, RoCoF measurement methodologies are very important and do result in different values. Moreover, 500 ms does not necessarily represent the highest or average RoCoF.

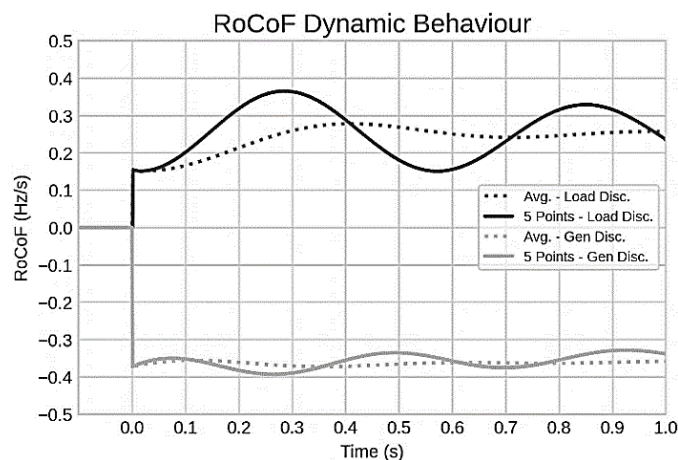


Figure 4. RoCoF dynamic behavior

#### 4. CONCLUSION

This paper proposed the PEM ( $2m+1$ ) for analyzing the probabilistic behavior of RoCoF when having a large renewable energy participation. Historical data allowed the statistical moments of WPPs to be used such as to calculate point concentrations with their corresponding weights for building a 95% confidence interval. Two cases were analyzed with the connection of one and two WPPs. Different scenarios were considered, such as type of power balance disturbance, and the correlation between WPPs.

One of the benefits of using PEM, and hence building a 95% confidence interval is that it is a useful way not only to know how RoCoF will behave, but also as a tool for comparisons between cases and scenarios. TSO's would be the most benefited from using PEM and confidence intervals, because reliable results can be achieved with a very low number of simulations, contrary to what would happen with Monte-Carlo simulations. It can also be used as a common platform from which values can be compared regardless of statistical behavior or number of random WPP power inputs.

Important results were reached such as the difference between load loss and generation loss, and the little reliance of RoCoF changes based on power setpoint. PEM also allows the reader to be aware of the changes that the RoCoF measurement methodology can have on the final results. As such, it is clear that RoCoF will be different according to the time of measurement and whether an averaging is considered or a numerical equation is used. Numerous further research can be developed on RoCoF and PEM, such as a random behavior of inertia connection, size of power balance disturbances and cases with larger amounts of WPPs, interfaced with both grid-following and grid-forming converters.

This investigation regarding the probabilistic behavior of RoCoF serves as a launching point for RoCoF analysis based on its confidence interval. As this paper has shown, it is not ideal to treat it as one crisp value. As such, further insights arise by treating system reliability and security as a probability. Other factors come to light when they have a random behavior. Load loss in practical applications is also not certain, and as such has a probability density function, which ultimately will impact RoCoF, the used PEM method is robust and can take this variation into account. Lastly, RoCoF measurement has been reported to be different between buses. As such, a bus electrically far away from generators and only supported by a WPP, may be exposed to higher RoCoF values than those in close connected buses. Quantifying this change in terms of a confidence interval could give us valuable information. Possible limitations in this line of research include availability of historical data in such volume as to have a trustful probability description. This applies to future expansion as to tie-line reactance, temperature, and size of load loss.

## REFERENCES

- [1] M. E. S. Mnguni and Y. D. Mfoumboulou, "An approach for a multi-stage under-frequency based load shedding scheme for a power system network," *International Journal of Electrical and Computer Engineering (IJECE)*, vol. 10, no. 6, pp. 6071–6100, Dec. 2020, doi: 10.11591/ijece.v10i6.pp6071-6100.
- [2] *Investigations on ROCOF withstand capability on large synchronous generators*. Paris, France: CIGRE Session, 2018.
- [3] M. G. Arcia, Z. G. Sanchez, H. H. Herrera, J. A. G. C. Cruz, J. I. S. Ortega, and G. C. Sánchez, "Frequency response analysis under faults in weak power systems," *International Journal of Electrical and Computer Engineering (IJECE)*, vol. 12, no. 2, pp. 1077–1088, Apr. 2022, doi: 10.11591/ijece.v12i2.pp1077-1088.
- [4] D. Doheny and M. Conlon, "Investigation into the local nature of rate of change of frequency in electrical power systems," in *2017 52nd International Universities Power Engineering Conference (UPEC)*, Aug. 2017, pp. 1–6, doi: 10.1109/UPEC.2017.8231982.
- [5] H. R. Chamorro, F. R. S. Sevilla, F. Gonzalez-Longatt, K. Rouzbehi, H. Chavez, and V. K. Sood, "Innovative primary frequency control in low-inertia power systems based on wide-area RoCoF sharing," *IET Energy Systems Integration*, vol. 2, no. 2, pp. 151–160, Jun. 2020, doi: 10.1049/iet-esi.2020.0001.
- [6] H. B. Lai, A.-T. Tran, V. Huynh, E. N. Amaefule, P. T. Tran, and V.-D. Phan, "Optimal linear quadratic Gaussian control based frequency regulation with communication delays in power system," *International Journal of Electrical and Computer Engineering (IJECE)*, vol. 12, no. 1, pp. 157–165, Feb. 2022, doi: 10.11591/ijece.v12i1.pp157-165.
- [7] J. Suh, J. Lee, S. Jung, and M. Yoon, "Imbalance-based primary frequency control for converter-fed microgrid," *IET Generation, Transmission and Distribution*, vol. 16, no. 2, pp. 247–256, Jan. 2022, doi: 10.1049/gtd2.12221.
- [8] B. S. Rameshappa and N. M. Shadaksharappa, "An optimal artificial neural network controller for load frequency control of a four-area interconnected power system," *International Journal of Electrical and Computer Engineering (IJECE)*, vol. 12, no. 5, pp. 4700–4711, Oct. 2022, doi: 10.11591/ijece.v12i5.pp4700-4711.
- [9] S. Rozada, D. Apostolopoulou, and E. Alonso, "Deep multi-agent reinforcement learning for cost-efficient distributed load frequency control," *IET Energy Systems Integration*, vol. 3, no. 3, pp. 327–343, Sep. 2021, doi: 10.1049/esi2.12030.
- [10] T. Kobayashi, K. Kawabe, and K. Tokumitsu, "A study on emergency control of battery energy storage systems for primary frequency regulation after unexpected loss of generation," *Electrical Engineering in Japan*, vol. 214, no. 4, Dec. 2021, doi: 10.1002/ej.23357.
- [11] N. Modi, A. Jalali, I. Commerford, and A. Groom, "Fast frequency response from transmission-connected solar farms: Australian experience," *Cigre Science and Engineering*, no. 24, pp. 187–199, 2022.
- [12] U. Akram, N. Mithulananthan, R. Shah, and S. A. Pourmousavi, "Sizing HESS as inertial and primary frequency reserve in low inertia power system," *IET Renewable Power Generation*, vol. 15, no. 1, pp. 99–113, Jan. 2021, doi: 10.1049/rpg2.12008.
- [13] M. Mohiti, M. Mazidi, M. Kermani, and D. A. Zarchi, "Frequency-constrained energy and reserve scheduling in wind incorporated low-inertia power systems considering vanadium flow redox batteries," *IET Generation, Transmission and Distribution*, Aug. 2022, doi: 10.1049/gtd2.12592.
- [14] A. Tavakoli, S. Saha, M. T. Arif, M. E. Haque, N. Mendis, and A. M. T. Oo, "Impacts of grid integration of solar PV and electric vehicle on grid stability, power quality and energy economics: a review," *IET Energy Systems Integration*, vol. 2, no. 3, pp. 243–260, Sep. 2020, doi: 10.1049/iet-esi.2019.0047.
- [15] M. Yesil and E. Irmak, "Estimation of inertia constant in Turkish power system and its analysis during real system disturbances," *International Transactions on Electrical Energy Systems*, vol. 31, no. 11, Nov. 2021, doi: 10.1002/2050-7038.13106.
- [16] A. Fernández-Guillamón, E. Gómez-Lázaro, and Á. Molina-García, "Extensive frequency response and inertia analysis under high renewable energy source integration scenarios: application to the European interconnected power system," *IET Renewable Power Generation*, vol. 14, no. 15, pp. 2885–2896, Nov. 2020, doi: 10.1049/iet-rpg.2020.0045.
- [17] B. Wang *et al.*, "Power system inertia estimation method based on maximum frequency deviation," *IET Renewable Power Generation*, vol. 16, no. 3, pp. 622–633, Feb. 2022, doi: 10.1049/rpg2.12367.
- [18] M. Kuivaniemi, N. Modig, and R. Eriksson, *Real-time estimation of frequency stability using a dynamic model tuned based on real events*. Paris, France: CIGRE Session, 2020.
- [19] Y. Wen, R. Zhao, M. Huang, and C. Guo, "Data-driven transient frequency stability assessment: A deep learning method with combined estimation-correction framework," *Energy Conversion and Economics*, vol. 1, no. 3, pp. 198–209, Dec. 2020, doi: 10.1049/enc2.12015.

- [20] B. O'connell, N. Cunniffe, M. Eager, D. Cashman, and J. O'sullivan, "Assessment of technologies to limit the rate of change of grid frequency on an island system," in *Proceedings of the CIGRE Technical Meeting, Paris, France*, 2018, pp. 26–31.
- [21] J. Fournel, G. Prime, and Y. Wang, *Assessment of the dynamic frequency stability of the future continental Europe power system-interconnected incidents and system splits*. Paris, France: CIGRE Session, 2020.
- [22] H. P. Hong, "An efficient point estimate method for probabilistic analysis," *Reliability Engineering and System Safety*, vol. 59, no. 3, pp. 261–267, Mar. 1998, doi: 10.1016/s0951-8320(97)00071-9.
- [23] R. Eriksson, N. Modig, and K. Elkington, "Synthetic inertia versus fast frequency response: a definition," *IET Renewable Power Generation*, vol. 12, no. 5, pp. 507–514, Nov. 2017, doi: 10.1049/iet-rpg.2017.0370.
- [24] O. Dudurych and M. Conlon, "Impact of reduced system inertia as a result of higher penetration levels of wind generation," *2014 49th International Universities Power Engineering Conference (UPEC)*, Sep. 2014, doi: 10.1109/upec.2014.6934801.
- [25] EirGrid/SONI, "RoCoF modification proposal-TSO's recommendations." EirGrid/SONI Dublin, Ireland, 2012.
- [26] *High fidelity modelling approach to analysing combined-cycle power plant response to proposed ROCOF requirements in ireland*. Paris, France: CIGRE Session.
- [27] W. Gautschi, "Numerical differentiation and integration," in *Numerical Analysis*, Birkhäuser Boston, 2011, pp. 159–251.
- [28] J. M. Morales, L. Baringo, A. J. Conejo, and R. Mínguez, "Probabilistic power flow with correlated wind sources," *IET Generation, Transmission & Distribution*, vol. 4, no. 5, 2010, doi: 10.1049/iet-gtd.2009.0639.
- [29] R. C. A. Ardila, "Probabilistic load flow in HVAC/HVDC systems with high participation of intermittent renewable energy sources." Universidad de los Andes, 2020.
- [30] A. C. Cepeda and M. A. Rios, "Bulk power system availability assessment with multiple wind power plants," *International Journal of Electrical and Computer Engineering (IJECE)*, vol. 11, no. 1, pp. 27–36, Feb. 2021, doi: 10.11591/ijece.v11i1.pp27-36.
- [31] W. Hines, D. Montgomery, D. Goldsman, and C. Borror, "Chapter 10: Parameter estimation," in *Probability and Statistics in Engineering*, 4th ed., Wiley: Hoboken, 2003, pp. 216–257.
- [32] M. Rampokanyo *et al.*, "Impact of high penetration of inverter-based generation on system inertia networks," *Electra*, 2021.
- [33] S. Hadavi, S. Me, B. Bahrani, M. Fard, and A. Zadeh, "Virtual synchronous generator versus synchronous condensers: a electromagnetic transient simulation-based comparison," *Cigre Science and Engineering*, 2022.
- [34] A. Tuckey and S. Round, "Practical application of a complete virtual synchronous generator control method for microgrid and grid-edge applications," in *2018 IEEE 19th Workshop on Control and Modeling for Power Electronics (COMPEL)*, Jun. 2018, pp. 1–6, doi: 10.1109/COMPEL.2018.8459987.
- [35] P. M. Anderson and A. A. Fouad, "Chapter 2: The elementary mathematical model," in *Power System Control and Stability*, 2nd Ed., Wiley: NJ, USA: IEEE Press, Wiley-Interscience, 2003, pp. 13–52.
- [36] R. A. Vergara and M. A. Rios, "Probabilistic model of wind power parks for reliability assessment," in *2020 IEEE ANDESCON*, Oct. 2020, pp. 1–5, doi: 10.1109/ANDESCON50619.2020.9272051.
- [37] S. Hinchliffe and J. Eggleston, *System strength, inertia and network loss factors-implications for power networks and renewable generation*. Paris, France: CIGRE Session, 2021.

## BIOGRAPHIES OF AUTHORS



**Tomas Rubiano**    received a degree in electrical engineering in 2022, from Universidad de los Andes, Bogota, Colombia. Currently, he is student of a Master of Science degree in Electrical Engineering at the Friedrich-Alexander Universität Erlangen-Nürnberg. His areas of interest are power electronics, high voltage technology, and industrial applications. He can be contacted at t.rubiano@uniandes.edu.co.



**Mario A. Rios**    received a degree in electrical engineering in 1991 and a M.Sc. degree in Electrical Engineering in 1992, both from Universidad de los Andes, Bogota, Colombia. He received a Ph.D. degree in Electrical Engineering from INPG-LEG, Grenoble, France, in 1998, and a doctoral degree in engineering from Universidad de los Andes, in 1998. He worked as a consultant engineer in ConCol (now WSP), Bogotá, Colombia, for 12 years. Also, he was a research associate at the University of Manchester (formerly, UMIST). Currently, he is full professor at the Department of Electrical Engineering, School of Engineering, Universidad de los Andes, Bogotá. He can be contacted at email: mrios@uniandes.edu.co.